PCCP

View Article Online / Journal Homepage / Table of Contents for this issue
Dynamic Article Links

Cite this: *Phys. Chem. Chem. Phys.*, 2011, **13**, 2044–2051

www.rsc.org/pccp

PAPER

Understanding the aggregation induced emission enhancement for a compound with excited state intramolecular proton transfer character†

Rui Hu,[a] Shayu Li,*[a] Yi Zeng,[b] Jinping Chen,[b] Shuangqing Wang,[a] Yi Li*[b] and Guoqiang Yang*[a]

Received 14th July 2010, Accepted 4th November 2010
DOI: 10.1039/c0cp01181a

A few of excited state intramolecular proton transfer (ESIPT) compounds have been discovered for their aggregation induced emission enhancement (AIEE). To understand the AIEE mechanism, an ESIPT compound BTHPB (*N*-(4-(benzo[d]thiazol-2-yl)-3-hydroxyphenyl)-benzamide) with simple structure was designed and synthesized. BTHPB showed apparent AIEE property and the emission efficiency was observed as high as 0.27 in the aggregates. On the basis of viscochromism experiments and calculations employing the linear coupling model, the restriction of the rotation between the two subunits taken place in ESIPT was considered as the main factor for the AIEE. The micro- and femtosecond transient absorption experiments offered evidence for the considerations. Additionally, we also observed a negative effect of aggregation on the fluorescence emission in the system. So the AIEE of ESIPT compound BTHPB originated from the combination effects of positive and negative factors induced by the aggregation.

1. Introduction

Luminescent organic aggregates such as amorphous solids, nano- or microcrystals are found to be much more photostable than isolated molecules.[1] On account of other advantages including facilitation of structural design, low cost, and unique properties, these aggregates have attracted considerable interest for their potential applications in fluorescence sensors, flat panel display and illumination, *etc.*[2–5] In all of these applications, luminescent intensity of the aggregates is a key factor to evaluate their performance and even predominantly determines their applicable extension. Unfortunately, most of the luminescent organic compounds are usually weak or even non-emitting in their solid state, in contrast to the strong fluorescence in their dilute solutions.[6] This behavior is generally attributed to the so-called concentration quenching effect in that nonradiative deactivation of the excited state is enhanced by strong intermolecular vibronic interactions such as exciton coupling and excimer formation in the solid state.[7,8]

Although to control the self-quenching or nonradiative processes in aggregates is still a challenge for the luminescent materials, much effort has been spent to mitigate these notorious effects and a few new luminogens that can emit efficiently in the aggregate state have been discovered.[9–11] Successful development was pioneered by Tang *et al.*, who synthesized a series of aromatic siloles that show unique enhanced emission rather than fluorescence quenching in aggregates.[12–17] Different type of compounds with aggregation induced emission enhancement (AIEE) characteristics have been reported by several research groups.[18–24] These compounds include aromatic siloles, arylethene derivatives, fluorenone excimers, dibenzosuberenylidene, diphenyldibenzofulvenes, pyran derivatives, as well as conjugation polymers *etc.* According to the structure of the compounds, the enhanced emission has been attributed to single or combined effects of molecular planarization, restricted group rotations in the molecules, prevention of exciton diffusion and *J*-aggregates formation.[25] To date, examples of the AIEE systems are still quite limited, especially concerning the enormously increasing number of luminescent organic compounds. So it is desirable to develop more compounds with AIEE for their application possibility.

We have developed a novel class of AIEE material, the excited state intramolecular proton transfer (ESIPT) compounds.[26] ESIPT compounds are of great interest from a basic research viewpoint as well as for their various applications.[27] Several ESIPT compounds have been applied in optic/optoelectronic devices, such as tunable solid-state lasers and organic light emitting devices (OLEDs).[28–30] In ESIPT compounds, an excited state tautomeric reaction

---

[a] *Beijing National Laboratory for Molecular Sciences, Key laboratory of Photochemistry, Institute of Chemistry, Chinese Academy of Sciences, Beijing 100190, China. E-mail: gqyang@iccas.ac.cn, shayuli@iccas.ac.cn; Fax: +86-10-82617315; Tel: +86-10-82617263*
[b] *Key Laboratory of Photochemical Conversion and Optoelectronic Materials, Technical Institute of Physics and Chemistry, Chinese Academy of Sciences, Beijing 100190, P. R. China. E-mail: yili@mail.ipc.ac.cn*

† Electronic supplementary information (ESI) available: Spectra and a SEM image. See DOI: 10.1039/c0cp01181a

concerning a proton transfer from a proton donor to an acceptor group occurs *via* an intramolecular H-bond or H-bonding bridge, which leads to an intrinsic peculiar four-level photophysical cycle (absorption-proton transfer-emission-back proton transfer) after photoexcitation.[31] As a result, an abnormal large Stokes shift is observed, which diminishes the self-absorption and renders the possibility of intense emission for these compounds in the solution with high concentration or aggregates. So ESIPT compounds are expected to be potential intrinsic luminescent materials.

In previous works, the mechanisms of AIEE for ESIPT compounds were preliminary investigated and explained as the effects of combining *J*-aggregation and restriction of intramolecular rotation. In this work, we extend our earlier study with several experimental and computational approaches to understand the AIEE process. A new ESIPT compound, *N*-(4-(benzo[d]thiazol-2-yl)- 3-hydroxyphenyl)benzamide (BTHPB), with AIEE feature was designed and synthesized. The flash photolysis and femtosecond transient absorption and calculations employing the linear coupling model were carried out to help us explore what is the most important factor for the emission enhancement behavior in the aggregates of ESIPT compounds.

Experimental

Materials

Benzoic acid and 1,1′-carbonyldiimidazole (CDI) were obtained from Beijing Chemical Reagents. Cyclohexane, paraffin oil, ethyl ether, CH_3CN and THF were AR grade received from ACROS. Polystyrene (PS) was obtained from ACROS. All chemicals were used directly without further purification.

Synthesis of BTHPB

2-(4-Amino-2-hydroxyphenyl)benzothiazole (AHBA) was synthesized according to ref. 32.

BTHPB (*N*-(4-(benzo[d]thiazol-2-yl)-3-hydroxyphenyl)-benzamide). The preparation procedure was performed according to ref. 33. 602 mg benzoic acid (5 mmol) and 0.972 g CDI (6 mmol) were mixed at a dry argon atmosphere in 30 ml toluene then refluxed for 6 h. When the temperature cooled down, 1.224 g AHBA (5 mmol) was added to the solution, the reaction system was stirred again and refluxed overnight. The deposit was collected with a good yield, and then purified by repeatedly washing with CH_2Cl_2/CH_3OH (V/V = 10:1) to give a white solid (yield 74%). ^{1}H-NMR(400 MHz, d_6-DMSO, ppm) δ = 11.67 (s, 1H), 10.48 (s, 1H), 8.13 (t, *J* = 8.92, 2H), 8.02 (d, *J* = 8.08, 1H), 7.98 (d, *J* = 7.28, 2H), 7.80 (d, *J* = 1.64, 1H), 7.64-7.51 (m, 4H), 7.42(t, *J* = 8.32, 2H). EI-MS (*m*/*z*): 346 (m^+). Anal. Calcd. for $C_{20}H_{14}N_2O_2S$: C, 69.35; H, 4.07; N, 8.09, found: C, 69.20; H, 4.11; N, 8.17. And the molecular structure were shown in Scheme 1.

Preparation of the aggregates

The aggregates of BTHPB in water were prepared by once injecting 50 μL THF solution (2.0×10^{-3} M) into 10 mL H_2O with vigorous stirring for 20 s at room temperature, then the solution was immediately taken for fluorescence, absorption and fluorescent decay detection.

Spectroscopy characterization

UV-vis absorption spectra were recorded on a Hitachi U-3010 spectrophotometer. Fluorescence spectra were recorded using a Hitachi F-4500 fluorescence spectrophotometer. The time-resolved fluorescence spectra and fluorescence lifetime were investigated with an Edinburgh FL900 spectrophotometer and a pulsed LED from 370 nm was used to excite the samples. The nanosecond transient absorption experiments were investigated by Edinburgh Instruments LP920. The excitation light was the harmonic of the Nd:YAG laser (Continuum Surelite, 355 nm and 7 ns fwhm). A pulsed xenon arc lamp was used to provide the analyzing light. The femtosecond transient absorption spectra were recorded with ExciPro pump–probe spectrometer. The pump light (170 fs, 360 nm, 1 kHz) was provided by a combination of Coherent Chameleon Ultra, Legend Elite and OPerA Solo. All the analyzed spectra were corrected for a chirp of a white light continuum.

Computational methods

Geometry optimization for the ground state of the BTHPB molecule was carried out using the TURBOMOLE suite with the density functional theory.[34,35] Becke's three-parameters hybrid method, using the Lee–Yang–Parr correlation functional (B3LYP), was employed here. The structures of the lowest excited state for BTHPB keto tautomer were obtained by TDDFT (time-dependent density functional theory) methods, employing the hybrid functional B3LYP. The calculations of vibration frequencies and normal coordinates were carried out at the TDDFT structure. Employing the linear coupling model, we investigated the major routes of internal conversion of the excited states. For all the above calculations we employed the 6-31G(d) basis set for carbon, hydrogen, oxygen, nitrogen, and sulfur atoms.

Results

Absorption and fluorescence spectroscopy

Solid BTHPB is soluble more or less in all conventional organic solvents. The absorption spectra of BTHPB in cyclohexane, ethyl ether, THF and CH_3CN at room temperature were shown in Fig. 1a and S1a.† The data in protic and halogen solvents were excluded to avoid specific solute–solvent interactions. From the spectra, it could be seen that the absorbance of BTHPB seldom changed in both shape and position with increasing the solvent polarity, which indicated that the BTHPB molecule had no apparent conjugation-structural changes in the ground state in different solvents. All absorption bands with maxima at ~350 nm were assigned to the π–π* transition that corresponded to the coupling between benzothiazole and the hydroxyphenyl ring.[26] The absorbance of BTHPB in water was also shown in Fig. 1a. The absorption band at ~350 nm decreased significantly probably due to the formation of large particles, which were in agreement with the SEM observations (see in Fig. S2).†

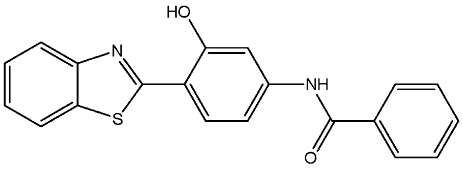

Scheme 1 Molecular structure of BTHPB.

The fluorescence spectra of BTHPB in various solvents were shown in Fig. 1b and S1b.† Unlike the absorbance changes, BTHPB fluorescence responses to solvents exhibited a moderate change in both shape and intensity. In cyclohexane, BTHPB showed one emission band with a maximum at 509 nm. In contrast, two emission bands peaking at 400 and 509 nm were observed in other polar solvents. As was well known, ESIPT compounds could form intermolecular H-bonds with protic or polar solvents, which interrupted the ESIPT process and induced a local emission from the enol form.[36] So the emission with a small Stokes shift, around 400 nm, was assigned from the enol excited state with intermolecular hydrogen bond configuration. With regard to the emission at 509 nm, the large Stokes shift indicated that it could be assigned to the ESIPT emission. It was worthwhile to note that almost no changes in both the energy region and the band shape of the ESIPT emission were observed with increasing the solvent polarity, suggesting that the excited state of *cis*-keto was the form without intramolecular charge transfer character. The fluorescence spectrum of BTHPB aggregates is shown in Fig. 1b. Similar to that in the cyclohexane solution, no enol but only ESIPT emission was observed. Additionally, the shapes of excitation spectra monitored at 509 nm (shown in Fig. S3†) resembled closely those of the absorption spectra either in cyclohexane or in aggregates, respectively. This indicated that all high-level excited states can only relax to the same lowest excited state.

Enhanced emission phenomenon

All the dilute solutions of BTHPB in four organic solvents presented weak fluorescence. Among them, BTHPB in cyclohexane gave the highest quantum efficiency, just only 0.018 (τ = 0.23 ns). The lower fluorescent quantum efficiencies in other polar solvents were probably induced by the intermolecular hydrogen bonds that decreased the number of molecules undergoing ESIPT reactions.[37] However, emission of BTHPB aggregates in water exhibited large a enhancement from its monodisperse solutions though energy and band shape were consistent. The luminescent quantum efficiency of BTHPB aggregates was as high as 0.27 (τ = 7.0 ns), which was nearly 15-fold higher than that of the solution in cyclohexane. The same emission energy and shape suggested that the fluorescence in cyclohexane and aggregates came from the transition between the same excited state and ground state structures of *cis*-keto form. The different quantum efficiency implied the different formation processes and/or radiationless decay routes of the excited states.

The quantum yield of the transition from enol* to *cis*-keto* was generally very high due to the ultrafast ESIPT process in comparison with other decay processes, and no enol emissions were observed in cyclohexane solution or aggregates. We thus mainly focused on the emission from the *cis*-keto* form in the following discussion.

Discussion

In general, AIEE should be achieved easily if the aggregation (i) resulted in protecting the fluorophore from fluorescence quenching that normally took place for the dissolved molecules (*e.g.* thermal motions, intersystem crossing), and (ii) mitigated nonradiative deactivation processes that normally took place in the aggregates (*e.g.* exciton coupling, exciton diffusion).[25] In the following section, the major routes of the radiationless decay process of monodisperse BTHPB were explored firstly, and then the effects of aggregation on nonradiative deactivation processes were discussed. And finally the origin of AIEE phenomena was investigated.

Nonradiative decay routes of monodisperse BTHPB

For the normal organic compounds, internal conversion (IC), intersystem crossing (ISC) from singlet state to triplet state, and energy transfer to surrounding molecules (ET) were three mainly possible nonradiative decay processes for the dissolved molecules.[38] When BTHPB molecules were dispersed in solvent, the absorbance of either cyclohexane or BTHPB itself was far from the emission band and located in high energy area, diminishing the possibility of ET with a trivial

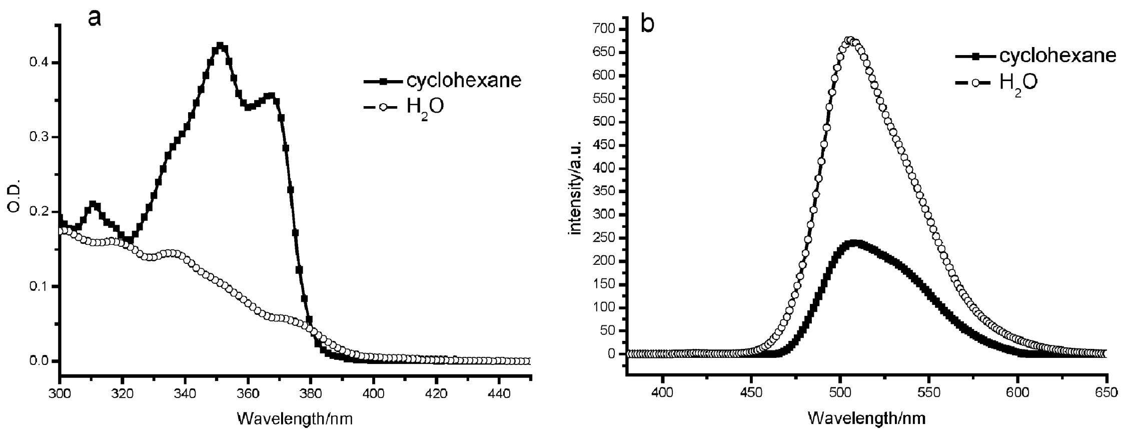

Fig. 1 Absorption and fluorescence spectra of BTHPB in cyclohexane and water. Concentration: 1.0 × 10^{-5} M. Excitation at 360 nm.

mechanism. And the average distance between two BTHPB was several tens of nanometres in the dilute solution, which prevented possible ET with Förster and Dexter mechanisms. So the ET process was rationally neglected. In addition, intersystem crossing was not important for the HBT-type compounds without heavy atoms at room temperature and the absence of apparent spin–orbit coupling effect.[39] Therefore the IC route was the major component of a nonradiative decay process for BTHPB solution. In the IC process, the energy of the electronically excited state was relaxed to various vibrational modes of the molecule, that is, torsions, rotations and vibrations served as nonradiative channels for the excited species to decay.[40] In general, only molecular torsions and rotations but not vibrations were restrained effectively by tight packing of the molecules. Thereby, the AIEE of BTHPB possibly originated from a restriction of molecular torsions and rotations.

To verify this hypothesis, BTHPB was dissolved in the solvents with different viscosities. Consideration was given to the thought that higher viscosity of the solvent could hamper the torsions and rotations of the molecules. Mixtures of cyclohexane and paraffin oil were chosen as the solvents to study the viscosity effect on the emission of BTHPB. As expected, the fluorescence of BTHPB, shown in Fig. 2b, was enhanced in turn with increasing the viscosity of the solvent while the absorbance was consistent, as shown in Fig. 2a. The emission quantum efficiency of BTHPB in paraffin oil (80% volume ratio) was calculated as 0.050, which was nearly 3-fold higher than that of cyclohexane solution. Taking the fact that the viscosity of paraffin oil was only 15.3 cP, much lower than that of normal organic soft-material,[41] the restrictions of the torsional and rotational motions would be much more apparent in the aggregates the viscosity of which was estimated reasonably to at least 10^{11} cP (pitch, 2.3×10^{11} cP).[42] Therefore, the restriction of the intramolecular motions played a key role for AIEE phenomena of BTHPB, similar to other AIEE compounds.

Although the restriction of torsions and rotations by tight packing in the aggregate was very important for the AIEE phenomenon, the main nonradiative channels for the excited species could not be deduced only from the fluorescent viscosity effects and thus remained unclear. In previous works, first-principles linear-coupling-model calculations had been proven as a reliable qualitative method more than a quantitative one to explore IC nonradiative decay processes.[43] Herein, we investigated the vibrational modes with noticeable displacement and reorganization energy.

Under the displaced harmonic approximation, applying the Born–Oppenheimer adiabatic approximation, the internal conversion radiationless rate was determined by the Huang-Rhys factor (see the theoretical details in ref. 44). The Huang-Rhys factor characterized the modification of vibrational quanta during transition from one electronic state to another, which was given as:

$$S_j = \frac{\omega_j \Delta Q_j^2}{2\hbar}$$

ΔQ_j was the displacement of jth normal mode, and ω_j was the vibrational frequency of jth normal mode. And the reorganization energy of jth normal mode was

$$\lambda_j = S_j \omega_j \hbar$$

In Table 1, the Huang-Rhys factor and the reorganization energy of the *cis*-keto excited-state tautomer between the S_1 and S_0 states with noticeable displacement were given.

The modes with frequency of 1372, 1373 and 1412 cm^{-1} had major contributions to the reorganization energy. This indicated that the three vibrations were the most efficient internal conversion deactive routes of *cis*-keto excited state. The first two modes were assigned to in-plane bending motions of C–H in the cyclohexadienone ring. The third mode represented a mixing of aromatic skeletal stretching vibration and C–N (amide) stretching vibration. Additionally, it could be seen from Table 1 that the other modes with large reorganization energy (>100 cm^{-1}) could be assigned to rotating, swing or bending motions, except the last mode that belonged to stretching vibration of N–H in the thiazole ring. It is worthwhile to note that the mode 19 cm^{-1} with large reorganization energy corresponded to rotation around the bond between dihydrobenzo[d]thiazole and the cyclohexadienone ring, as shown in Fig. 3. The huge Huang-Rhys factor of this mode suggested that the rotation also contributed largely to the IC process.[43] As mentioned above, only rotations and

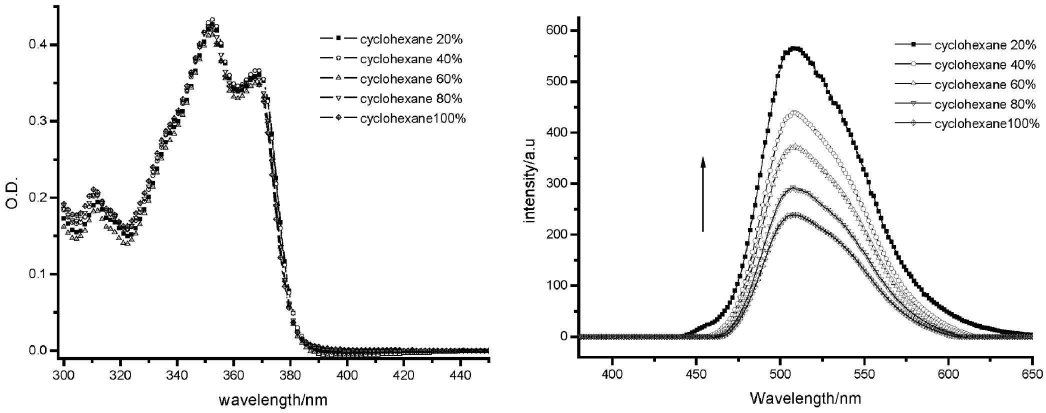

Fig. 2 Absorption and fluorescence spectra of BTHPB in mixtures of cyclohexane and paraffin oil. Concentration: 1.0×10^{-5} M. Excitation at 360 nm.

Table 1 Huang-Rhys factor and the reorganization energy for the noticeable displaced vibration modes of *cis*-keto tautomer of BTHPB

$\omega_j/\mathrm{cm}^{-1}$	S_j	$\lambda_j/\mathrm{cm}^{-1}$
19	13.12	245
112	0.4622	51
214	0.747	159
303	0.2895	87
317	0.2068	65
532	0.3321	176
561	0.211	118
987	0.2261	223
1099	0.1236	135
1118	0.0683	76
1132	0.0609	68
1248	0.0769	96
1312	0.0739	96
1372	0.3156	433
1373	0.2496	342
1412	0.5699	805
1495	0.1136	169
1497	0.0773	115
3138	0.0934	293

torsions could be constrained effectively by packing, thereby we considered that the restriction of intramolecular motions, especially the rotation of the two subunits which took place in the ESIPT process was the main cause for AIEE.

Aggregation effects on nonradiative decay processes

The generally accepted ESIPT mechanism of HBT-type ESIPT compounds is shown in Scheme 2. After the ESIPT, *cis*-keto* relaxed with two competitive processes: radiative decay to the *cis*-keto ground state and nonradiative decay to the *trans*-keto photoproduct.[45–49] The *cis*-keto species returned rapidly through ground state intramolecular proton transfer (GSIPT) to the initial enol tautomer and completed the four-level photophysical cycle, whereas *the trans*-keto photoproduct was stable from a few tens of microseconds to milliseconds.[50] We noted that the *trans*-keto form was transformed from the *cis*-keto form by rotating 180° *via* a bond between the dihydrobenzo[d]thiazole group and the cyclohexadienone ring. The rotation was considered the main nonradiative decay route, as mentioned in the previous discussion. Therefore, the block to rotation or not was expected to be expressed by number changes of *trans*-keto photoproduct. Transient absorption with flash photolysis experiments were thus carried out to check our considerations.

As shown in Fig. 4, transient absorption spectra of BTHPB in cyclohexane exhibited a positive band from 400 to 500 nm with a maximum at 450 nm. The band lifetime was too long to relax to zero in our instrument and could only be estimated as $\sim$500 μs at all wavelengths. These decay kinetics were insensitive to the presence of oxygen and thus could not be assigned to a triplet state. By analogy with other ESIPT compounds, the transient signals were attributed to the absorbance of a *trans*-keto photoproduct.[51] This absorption from the transient photoproduct proved that the rotation between the dihydrobenzo[d]thiazole group and the cyclohexadienone ring was present in the cyclohexane solution. In the aggregates, however, no transient absorption signals were detected, suggesting the restriction of the rotation by the physical constraint in the rigid matrix. The transient absorption measurements thus offered a solid experimental support to our consideration that the restriction of the rotation between the two subunits that took place in the ESIPT process was mainly responsible for the AIEE.

Fig. 3 Normal mode displacement vectors of the vibration mode 19 cm^{-1}.

To further investigate the difference of the ESIPT cycle between the solution and the aggregate, femtosecond transient absorption was also carried out. It was well-accepted that the solvent had no effects on the ESIPT process and on the efficiency of the creation of photochromic tautomers.[52] We thus chose THF (as a better solvent for BTHPB) and a polystyrene matrix instead of cyclohexane and aggregates (bad signal/noise ratio), respectively, because of the limitation of the detection sensitivity.

Spectral traces selected for several time delays between the pump and probe were shown in Fig. 5. During short time, two positive bands and an obvious negative band were observed in the BTHPB solution. The positive absorption band around 660 nm was generated as the same time with the negative band. The kinetic curve (see in Fig. S5†) was well fitted with the convolution of the instrumental function at the probe wavelength of 660 nm, showing a mono-exponential decay with a lifetime of 40 ps. According to the literature, it was assigned to the absorbance of S_1 (π,π^*) *cis*-keto state.[51] The decay kinetic curve (shown in Fig. S5†) of the negative band was well fitted with a 38 ps mono-exponential decay that was quite consistent with the lifetime of S_1 keto state as mentioned above. Additionally, because the position of the residual negative band was close to the steady-state emission, it was assigned to the stimulated emission from S_1 (π,π^*) of the *cis*-keto form. Further analysis of the decay curve indicated that the formation of the stimulated emission band was very fast even within the time range of the instrument function. This ultrafast process was commonly regarded as ESIPT process. Another positive band in the 440–500 nm range was assigned to the absorbance of the *trans*-keto photoproduct, which remained nearly constant after its generation during our measurement time range. Quite different from that in BTHPB solution, only two absorption bands of BTHPB were observed in the polystyrene matrix: the negative band around 510 nm and the positive band at 660 nm. The absorption in the range of 440–500 nm of the *trans*-keto photoproduct was not detected. Similar to the results of the flash photolysis experiment, the femtosecond absorption spectra also confirmed that the *trans*-keto photoproduct was only formed in the solution but not in the solid matrix, suggesting no generation of *trans*-keto tautomer occurred.

All the experimental and calculation results described above proved that the AIEE of BTHPB was originated from the restriction of the intramolecular rotation process. However, aggregation was not only a random packing process and the

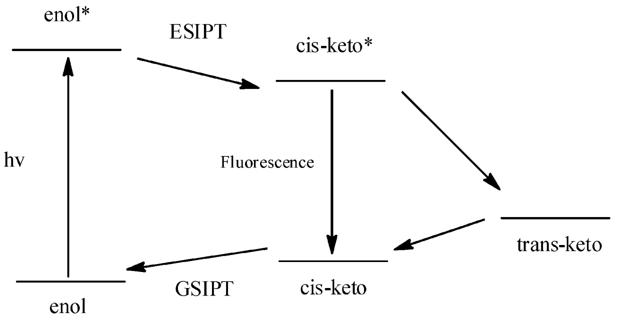

Scheme 2 Mechanism of a photoinduced process for HBT-type ESIPT compounds.

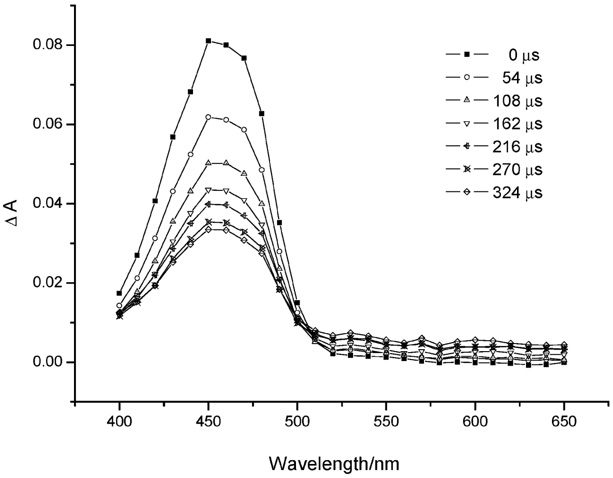

Fig. 4 Time-resolved transient absorption of BTHPB in cyclohexane, monitored by Edinburgh Instruments LP920.

molecules located in aggregates could not be considered simply as in a rigid matrix. As mentioned above, aggregation induced the emission up to 15-fold enhancement. On the other hand, we noticed that the fluorescent lifetime from *cis*-keto* increased about 30-fold (from 0.23 ns to 7.0 ns) after the aggregation process.

On the basis of photophysical principles and the specific four-level photophysical cycle of ESIPT compounds, the quantum efficiency of the *cis*-keto* emission should be expressed as:

$$\Phi = \Phi_{\mathrm{ESIPT}} \times \Phi_{F(K)} = \Phi_{\mathrm{ESIPT}} \times k_{F(K)} \times \tau_{F(K)} \qquad (1)$$

Thus, the ratio of quantum efficiency for BTHPB in the solution and the aggregates could be predicted as:

$$\frac{\Phi^{\mathrm{aggr}}}{\Phi^{\mathrm{sol}}} = \frac{\Phi^{\mathrm{aggr}}_{\mathrm{ESIPT}}}{\Phi^{\mathrm{sol}}_{\mathrm{ESIPT}}} \times \frac{\tau^{\mathrm{aggr}}_{F(K)} \times k^{\mathrm{aggr}}_{F(K)}}{\tau^{\mathrm{sol}}_{F(K)} \times k^{\mathrm{sol}}_{F(K)}} \qquad (2)$$

The inherent radiation decay rate k_F could be estimated, derived by the equation $k_f = f \times E^2/1.4992$, by using the Einstein spontaneous emission coefficient, where f and E were the oscillator strength and the energy of excited state, respectively.[44] Taking into account the fact that both fluorescence energy and spectra shape of *cis*-keto emission were consistent in aggregates and solutions, the oscillator strength and energy of *cis*-keto* could be considered as identical in both condensed states. In this case, eqn (2) could be simplified. After substituting Φ and τ into the equation, the relationship between $\Phi^{\mathrm{aggr}}_{\mathrm{ESIPT}}$ and $\Phi^{\mathrm{sol}}_{\mathrm{ESIPT}}$ was expressed as: $\Phi^{\mathrm{sol}}_{\mathrm{ESIPT}} \approx 2\Phi^{\mathrm{aggr}}_{\mathrm{ESIPT}}$, suggesting that the aggregation process induced the decrease of the ESIPT yield.

In general, ESIPT was an extremely fast process that k_{ESIPT} is about 10^{13} s^{-1} in solution and 10^{12} s^{-1} in the aggregates. Neither the radiative decay (rate constant is about 10^8–10^9 s^{-1}) nor internal conversion (rate constant is about 10^9–10^{10} s^{-1}) was able to compete effectively with the ESIPT process.[53] The mechanism of a decay process fast enough to compete with ESIPT was not very clear for the BTHPB aggregates. Taking the fact that the spectrum overlap of absorbance and emission of the enol tautomer was very small, the common exciton diffusion with the Förster mechanism could be excluded. Herein, we presumed that the decrease of Φ_{ESIPT} resulted from the strong intermolecular interactions of the enol forms in aggregates on account of the considerable changes of absorbance in the aggregates.[18,54]

Thus, two opposite effects were observed by the aggregation: (i) the intermolecular interactions induced a slight decrease of Φ_{ESIPT}, and (ii) restricted intramolecular rotation induced an increase of $\Phi_{F(K)}$. The combination of the

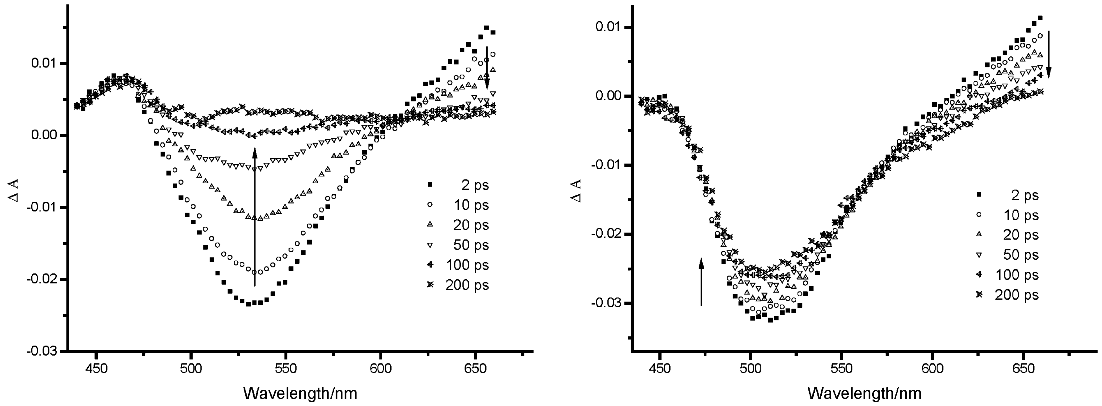

Fig. 5 Time-resolved transient absorption of BTHPB in (a) THF and in (b) polystyrene with 360 nm excitation, monitored by pump–probe setups.

two effects led to a significant emission enhancement in the BTHPB aggregates.

Conclusion

Although there are several reports on the AIEE behavior of organic compounds, there have been few works focusing on the AIEE mechanism of the ESIPT molecule. The novel ESIPT compound BTHPB presented an obvious AIEE phenomenon. With the viscosity effects, micro- and femtosecond transient absorption experiments and quantum chemical calculations, the predominant factor of AIEE for BTHPB was determined to the restriction of the rotation between the dihydrobenzo[d]thiazole group and the cyclohexadienone ring that undertook the ESIPT process. The negative factor induced by the aggregation was assigned to the intermolecular interactions. It indicated that the efficiency of the ESIPT process could not be simply assumed as 100% and the total AIEE observation is the combination of the positive and negative effects. The results implied that designing luminescent compounds with higher emission efficiency in the solid (or aggregates) should be balanced by the intermolecular interactions.

Acknowledgements

We are grateful to the National Natural Science Foundation of China (Grant Nos. 20703049, 20733007, 20873165, 50973118) and the National Basic Research Program (2007CB808004, 2009CB930802).

References

1 Y. N. Hong, J. W. Y. Lam and B. Z. Tang, *Chem. Commun.*, 2009, 4332–4353.
2 W. Chen, J. O. Bovin, A. G. Joly, S. P. Wang, F. H. Su and G. H. Li, *J. Phys. Chem. B*, 2004, **108**, 11927–11934.
3 A. Hagfeldt and M. Gratzel, *Chem. Rev.*, 1995, **95**, 49–68.
4 J. Y. Kim and F. E. Osterloh, *J. Am. Chem. Soc.*, 2005, **127**, 10152–10153.
5 A. N. Shipway, E. Katz and I. Willner, *ChemPhysChem*, 2000, **1**, 18–52.
6 B. K. An, S. K. Kwon, S. D. Jung and S. Y. Park, *J. Am. Chem. Soc.*, 2002, **124**, 14410–14415.
7 J. B. Birks, *in Photophysics of Aromatic Moelcules*, Wiley, London, 1970.
8 J. B. Birks and M. Leite, *J. Phys. Pt. B*, 1970, **3**, 513.
9 R. Deans, J. Kim, M. R. Machacek and T. M. Swager, *J. Am. Chem. Soc.*, 2000, **122**, 8565–8566.
10 W. Holzer, A. Penzkofer, R. Stockmann, H. Meysel, H. Liebegott and H. H. Hörhold, *Polymer*, 2001, **42**, 3183–3194.
11 C. Belton, D. F. O'Brien, W. J. Blau, A. J. Cadby, P. A. Lane, D. D. C. Bradley, H. J. Byrne, R. Stockmann and H. H. Horhold, *Appl. Phys. Lett.*, 2001, **78**, 1059–1061.
12 J. D. Luo, Z. L. Xie, J. W. Y. Lam, L. Cheng, H. Y. Chen, C. F. Qiu, H. S. Kwok, X. W. Zhan, Y. Q. Liu, D. B. Zhu and B. Z. Tang, *Chem. Commun.*, 2001, 1740–1741.
13 J. W. Chen, C. C. W. Law, J. W. Y. Lam, Y. P. Dong, S. M. F. Lo, I. D. Williams, D. B. Zhu and B. Z. Tang, *Chem. Mater.*, 2003, **15**, 1535–1546.
14 J. W. Chen, H. Peng, C. C. W. Law, Y. P. Dong, J. W. Y. Lam, I. D. Williams and B. Z. Tang, *Macromolecules*, 2003, **36**, 4319–4327.
15 J. W. Chen, B. Xu, X. Y. Ouyang, B. Z. Tang and Y. Cao, *J. Phys. Chem. A*, 2004, **108**, 7522–7526.
16 H. Tong, Y. Q. Dong, M. Haussler, J. W. Y. Lam, H. H. Y. Sung, I. D. Williams, J. Z. Sun and B. Z. Tang, *Chem. Commun.*, 2006, 1133–1135.
17 A. J. Qin, C. K. W. Jim, Y. H. Tang, J. W. Y. Lam, J. Z. Liu, F. Mahtab, P. Gao and B. Z. Tang, *J. Phys. Chem. B*, 2008, **112**, 9281–9288.
18 F. Wang, M. Y. Han, K. Y. Mya, Y. B. Wang and Y. H. Lai, *J. Am. Chem. Soc.*, 2005, **127**, 10350–10355.
19 J. Dong, K. M. Solntsev and L. M. Tolbert, *J. Am. Chem. Soc.*, 2009, **131**, 662–670.
20 H. Tong, Y. Q. Dong, Y. N. Hong, M. Haussler, J. W. Y. Lam, H. H. Y. Sung, X. M. Yu, J. X. Sun, I. D. Williams, H. S. Kwok and B. Z. Tang, *J. Phys. Chem. C*, 2007, **111**, 2287–2294.
21 H. Tong, Y. Dong, M. Haussler, Y. Hong, J. W. Y. Lam, H. H. Y. Sung, I. D. Williams, H. S. Kwok and B. Z. Tang, *Chem. Phys. Lett.*, 2006, **428**, 326–330.
22 K. Itami, Y. Ohashi and J. Yoshida, *J. Org. Chem.*, 2005, **70**, 2778–2792.
23 Z. X. Wang, H. X. Shao, J. C. Ye, L. Tang and P. Lu, *J. Phys. Chem. B*, 2005, **109**, 19627–19633.
24 Y. Liu, X. T. Tao, F. Z. Wang, X. N. Dang, D. C. Zou, Y. Ren and M. H. Jiang, *J. Phys. Chem. C*, 2008, **112**, 3975–3981.
25 J. F. Lamère, N. Saffon, I. Dos Santos and S. Fery-Forgues, *Langmuir*, 2010, **26**, 10210–10217.
26 Y. Qian, S. Y. Li, G. Q. Zhang, Q. Wang, S. Q. Wang, H. J. Xu, C. Z. Li, Y. Li and G. Q. Yang, *J. Phys. Chem. B*, 2007, **111**, 5861–5868.
27 S. J. Lim, J. Seo and S. Y. Park, *J. Am. Chem. Soc.*, 2006, **128**, 14542–14547.
28 S. Park, J. Seo, S. H. Kim and S. Y. Park, *Adv. Funct. Mater.*, 2008, **18**, 726–731.
29 K. Sakai, T. Tsuzuki, Y. Itoh, M. Ichikawa and Y. Taniguchi, *Appl. Phys. Lett.*, 2005, **86**, 081103.
30 S. M. Chang, Y. J. Tzeng, S. Y. Wu, K. Y. Li and K. L. Hsueh, *Thin Solid Films*, 2005, **477**, 38–41.
31 P. K. Sengupta and M. Kasha, *Chem. Phys. Lett.*, 1979, **68**, 382–385.
32 B. Ermanno, S. Piero, M. Mario and P. Macro, *J. Heterocycl. Chem.*, 1983, **20**, 1517–1521.
33 M. K. Chmielewski, V. Marchan, J. Cieslak, A. Grajkowski, V. Livengood, U. Munch, A. Wilk and S. L. Beaucage, *J. Org. Chem.*, 2003, **68**, 10003–10012.
34 P. Deglmann, F. Furche and R. Ahlrichs, *Chem. Phys. Lett.*, 2002, **362**, 511–518.
35 P. Deglmann and F. Furche, *J. Chem. Phys.*, 2002, **117**, 9535–9538.
36 A. S. Klymchenko, V. G. Pivovarenko and A. P. Demchenko, *J. Phys. Chem. A*, 2003, **107**, 4211–4216.
37 S. Y. Li, Q. Wang, Y. Qian, S. Q. Wang, Y. Li and G. Q. Yang, *J. Phys. Chem. A*, 2007, **111**, 11793–11800.
38 N. J. Turro, in *Modern Molecular Photochemistry*, Benjamin Cummings Publishing, Menlo Park, CA, 1978, ch. 9.
39 W. Al Soufi, K. H. Grellman and B. Nickel, *Chem. Phys. Lett.*, 1990, **174**, 609–616.
40 M. Bixon and J. Jortner, *J. Chem. Phys.*, 1968, **48**, 715–726.
41 P. E. Baillagou and D. S. Soong, *Polym. Eng. Sci.*, 1985, **25**, 232–244.
42 R. Edgeworth, B. J. Dalton and T. Parnell, *Eur. J. Phys.*, 1984, **5**, 198–200.
43 Q. Peng, Y. P. Yi, Z. G. Shuai and J. S. Shao, *J. Am. Chem. Soc.*, 2007, **129**, 9333–9339.
44 S. W. Yin, Q. Peng, Z. Shuai, W. H. Y. Fang, Y. H. Wang and Y. Luo, *Phys. Rev. B: Condens. Matter Mater. Phys.*, 2006, **73**, DOI: 10.1103/PhysRevB.73.205409.
45 W. E. Brewer, M. L. Martinez and P. T. Chou, *J. Phys. Chem.*, 1990, **94**, 1915–1918.
46 M. A. Ríos and M. C. Ríos, *J. Phys. Chem. A*, 1998, **102**, 1560–1567.
47 R. de Vivie-Riedle, V. De Waele, L. Kurtz and E. Riedle, *J. Phys. Chem. A*, 2003, **107**, 10591–10599.
48 A. J. A. Aquino, H. Lischka and C. Hättig, *J. Phys. Chem. A*, 2005, **109**, 3201–3208.
49 S. R. Vázquez, M. C. R. Rodríguez, M. Mosquera and F. Rodríguez-Prieto, *J. Phys. Chem. A*, 2007, **111**, 1814–1826.

50 M. Barbatti, A. J. A. Aquino, H. Lischka, C. Schriever, S. Lochbrunner and E. Riedle, *Phys. Chem. Chem. Phys.*, 2009, **11**, 1406–1415.
51 M. Sliwa, N. Mouton, C. Ruckebusch, S. Aloise, O. Poizat, G. Buntinx, R. Metivier, K. Nakatani, H. Masuhara and T. Asahi, *J. Phys. Chem. C*, 2009, **113**, 11959–11968.
52 M. Ziółek, J. Kubicki, A. Maciejewski, R. Naskręcki and A. Grabowska, *J. Chem. Phys.*, 2006, **124**, 124518.
53 B. Valeur, in *Molecular Fluorescence - Principles & Applications*, John Wiley and Sons Ltd., 2002.
54 Y. Kawamura, J. Brooks, J. J. Brown, H. Sasabe and C. Adachi, *Phys. Rev. Lett.*, 2006, **96**, DOI: 10.1103/PhysRevLett.96.017404.